Sensors and Actuators B 209 (2015) 252–257

Contents lists available at ScienceDirect

Sensors and Actuators B: Chemical

journal homepage: www.elsevier.com/locate/snb

Humidity sensing properties of $K_{0.5}Na_{0.5}NbO_3$ powder synthesized by metal organic decomposition

Mengjiao Yuan, Yong Zhang*, Xuejun Zheng, Bin Jiang, Peiwen Li, Shuifeng Deng

School of Physics and Optoelectronics, Xiangtan University, Xiangtan 411105, PR China

ARTICLE INFO

Article history:
Received 6 August 2014
Received in revised form
20 November 2014
Accepted 25 November 2014
Available online 3 December 2014

Keywords:
$K_{0.5}Na_{0.5}NbO_3$ powder
Humidity sensing properties
Dissipation factor
Complex impedance plots

ABSTRACT

$K_{0.5}Na_{0.5}NbO_3$ (KNN) powder is synthesized via a metal-organic decomposition (MOD) method and characterized by X-ray diffraction (XRD), field-emission scanning electron microscopy (FE-SEM), and energy dispersive spectrometer (EDS). A humidity sensor, which is consisted of five pairs of Ag—Pd interdigitated electrodes and an Al_2O_3 ceramic substrate, is fabricated by spin-coating the KNN powder on the substrate. The humidity sensing properties of the KNN humidity sensor are investigated at room temperature within the relative humidity (RH) range of 11–95%. The variations of the KNN humidity sensor impedance are about four orders of magnitude within the whole humidity range from 11% to 95% RH at the frequencies of 60 Hz and 100 Hz. The response time and recovery time of the KNN humidity sensor are all about 8 s and 18 s, and their maximum hystereses are all around 2% RH at 60 Hz and 100 Hz. Furthermore, at low RH and frequency conditions, the dielectric dissipation factor (DF) values of the KNN humidity sensor are small and hardly change, indicating that the KNN humidity sensor is of good insulating properties and reliability. The KNN powder is of broader potential applications for fabricating high performance humidity sensors.

1. Introduction

In recent years, measurement and controlling environmental humidity are of great importance in industry, agriculture, meteorology and human activities, and the humidity sensors have gained considerable attention [1–5]. More and more researchers are increasing paying their attention to exploitation of new materials in order to acquire humidity sensors with excellent properties such as linear response, higher sensitivity, wider humidity detection range and fast response speed [6–10]. Perovskite ABO_3-type complex metal oxides, an important material family for electronic and information technology, are also promising candidates for humidity sensors [2]. $K_{0.5}Na_{0.5}NbO_3$ (KNN) is a perovskite ABO_3-type complex metal oxide with the substitution of A-site ions. KNN is known to be a ceramic ferroelectric material with a higher Curie temperature [11–13]. KNN thin films have been widely studied because of their high Curie temperature and lead-free chemical composition [14–16]. KNN ceramics have also been recognized as promising piezoelectric materials for wide applications [16–18]. However, to the best of our knowledge, relatively few reports for the humidity sensing properties of KNN powder are available in the literatures.

The operating frequency is considered as an important parameter of humidity sensor by many researchers and it is generally about 100 Hz in previous work [19–22]. Zheng et al. reported the humidity sensing properties of A-site substituted Bi(Na, K)TiO_3 powder humidity sensor, and it was difficult to get the electric signal at the frequency under 100 Hz because of the high impedance [5]. Wang et al. reported that the impedance of the ZnO/TiO_2 humidity sensor was above 100 MΩ when the frequency was lower than 100 Hz, which was difficult to test [3]. Because of the appearance of skin effect in humidity sensing film at high frequency, the impedance of humidity sensor and the loss power are both increasing, which affect the humidity sensitivity and accuracy of humidity sensor [23,24]. Therefore, the low and wide working frequency range is benefit for the development of high performance humidity sensor.

Based on the previous researches [4,5,25,26], the humidity sensing properties of materials co-doped by K^+ and Na^+ are better than it only doped by K^+ or Na^+. In this paper, promoted by the distinct properties of KNN powder and its potential applications in humidity sensor, the KNN powder is synthesized by metal-organic decomposition (MOD) method, and the crystalline structures and morphologies of KNN powder are characterized by X-ray diffraction (XRD), field-emission scanning electron microscopy (FE-SEM) and energy dispersive spectrometer (EDS). The humidity sensor is

* Corresponding author. Tel.: +86 731 58292197.
E-mail address: zhangyong@xtu.edu.cn (Y. Zhang).

http://dx.doi.org/10.1016/j.snb.2014.11.118
0925-4005/

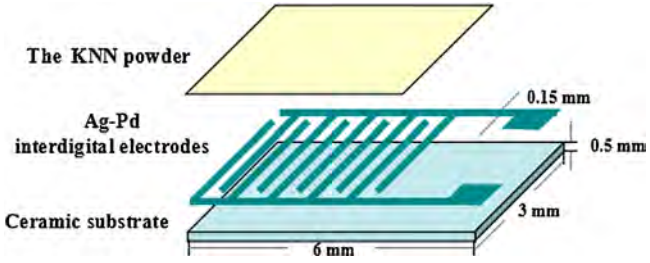

Fig. 1. A schematic diagram of the humidity sensor structure.

fabricated by coating the KNN powder on the substrate. The humidity sensing properties are investigated at different relative humidity (RH). We expect the results may offer useful guidelines to fabricate high performance humidity sensors which are of low and wide working frequency range.

2. Experimental details

2.1. Preparation and characterization of KNN powder

The KNN powder was synthesized by MOD method. The precursor solution was prepared by mixing potassium acetate, sodium acetate, and niobium ethoxide in 2-methoxyethanol solvent. In this case, 10 mol% excess amounts of K and Na alkoxides were added to compensate for their loss due to their volatility during heating [16]. And the final concentration of mixed solution was 0.30 mol/L. The above mixture was stirred for 12 h to promote the dissolution and reaction, and then kept for 12 h to gain the stable solution. The precursor solution was annealed at 650 °C for 3 h to obtain white powder. The powder was washed with deionized water and ethanol successively, and dried at 60 °C in air for further characterization. The crystalline structure of KNN powder was identified by XRD using a Bruker-AXS model D8-ADVANCE with Cu Kα ($\lambda = 0.15418$ nm). FE-SEM images were performed on a Carl Zeiss LEO1525 microscope with an accelerating voltage of 20 kV.

2.2. Fabrication and measurement of the humidity sensor

Fig. 1 shows a schematic diagram of the humidity sensor structure. The KNN powder was mixed with deionized water in a weight ratio of 100:25 to form a paste. The paste was spin-coated onto an Al_2O_3 ceramic substrate (6 mm × 3 mm, 0.5 mm in thick) with five pairs of Ag—Pd interdigitated electrodes (electrodes width and distance: 0.15 mm) to form a sensing film, and then the film was dried in air at 60 °C for 5 h. Finally, the humidity sensor based on KNN powder was obtained after aging at 95% RH with a voltage of 1 V, 100 Hz for 24 h to improve its stability and durability [27].

The humidity sensing properties of the KNN humidity sensor were measured on CHS-1 intelligent humidity sensitive analysis system (Beijing Elite Technology Co., Ltd.). The AC voltage applied was 1 V, and the frequency varied from 40 Hz to 100 kHz. The controlled humidity environments were achieved with supersaturation aqueous solutions of different salts in a closed glass vessel at room temperature, including LiCl, $MgCl_2$, $Mg(NO_3)_2$, NaCl, KCl, and KNO_3, which yielded 11, 33, 54, 75, 85 and 95% RH, respectively [28]. It took 10 h for the air in the glass vessel to reach equilibrium state in the investigations. The response time and recovery time were defined as the time taken by a sensor to achieve 90% of the total impedance change in the case of adsorption and desorption [29,30]. The hysteresis was measured by switching the humidity sensor between the chambers of 11%, 33%, 54%, 75%, 85% and 95% RH, and then shifting back. The RH of laboratory atmosphere was maintained at 25% RH by using an automatic drier. All of the sensing measurements were performed at a constant temperature of 25 °C.

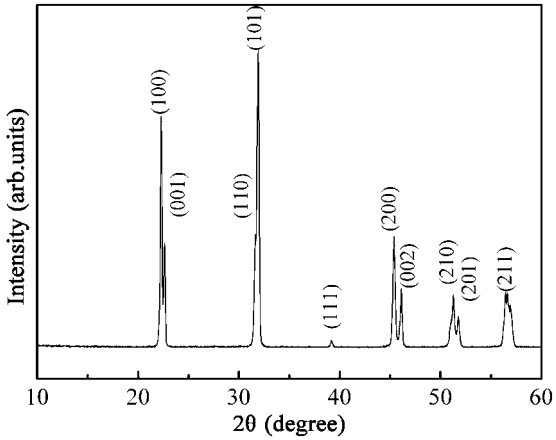

Fig. 2. XRD pattern of the KNN powder.

3. Results and discussion

3.1. Morphology and structure analysis

The crystalline structure of the powder obtained by sintering the KNN precursor solution is performed on XRD, and the XRD pattern is shown in Fig. 2. It can be noted that the XRD pattern reveals a single perovskite phase without any trace of secondary phase. The appearance of perovskite phase confirms that the homogeneous solid solution KNN is successfully formed [31], and the result of the XRD pattern is completely consistent with it of Sakamoto et al. [16]. In addition, the diffraction peaks are intensive and narrow which show that the powder obtained by sintering the KNN precursor solution is of good crystal quality [16,32,33].

The morphologies and composition of KNN powder are displayed in Fig. 3. It can be clearly seen that the KNN powder is of cuboid microstructure with diameters of 2–5 μm. Furthermore, as can be seen from Fig. 3(a), there are many fragments attached on the surface of each cuboid microstructure. The appearance of the fragments may be helpful for the increase of the specific surface, which may be quite useful for the water molecule adsorption and beneficial to its sensing properties. As shown in Fig. 3(b), the ratios of K/Na/Nb/O are approximately equal to the proportions of KNN, and the slight difference of element proportions is due to the volatilization of K^+ ion and Na^+ ion during the annealing process [34].

3.2. Humidity sensing properties

To find out the optimal relationship between impedance and RH of the humidity sensor based on KNN powder, the impedance vs. RH curves are measured at different frequencies (from 40 Hz to 100 kHz) and the results are shown in Fig. 4. We can see that the impedance of the KNN humidity sensor is obviously influenced by the frequency. The impedance decreases with increasing frequency in all RH range. The high humidity sensitivity and good linearity in the whole RH range are obtained when the frequency is 60 Hz and 100 Hz, and the impedance changes are about four orders of magnitude within the whole humidity range from 11% to 95% RH. At low RH, the impedance curves turn flat at high frequency, which indicates that the impedance of the KNN humidity sensor becomes independent of RH. This is because the electrical field direction changes fast at high frequencies and the polarization of water cannot catch up with it, resulting in the capacitance and

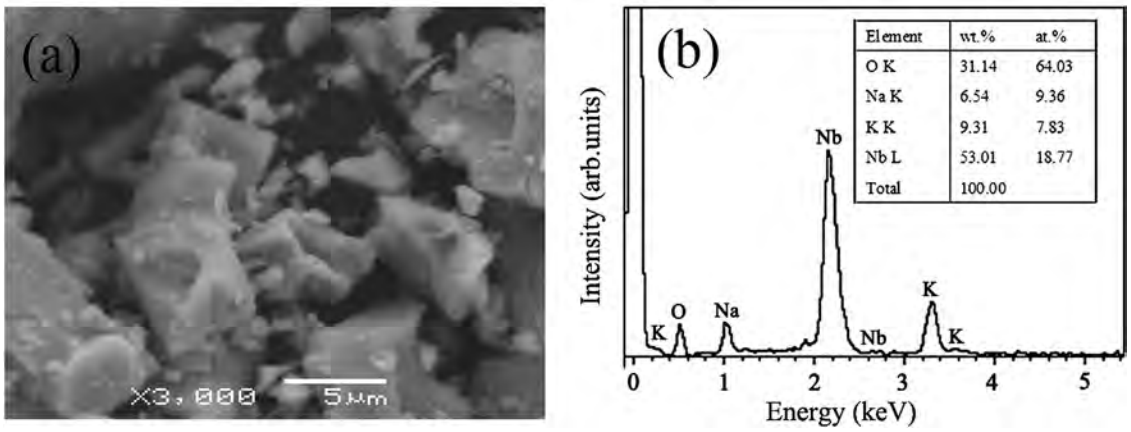

Fig. 3. (a) FE-SEM image of the KNN powder and (b) EDS pattern of the KNN powder.

the dielectric constant of the KNN humidity sensor being small and independent of the RH [35,36].

As a significant characteristic parameter of humidity sensor, the linearity is used to estimate the performance of humidity sensor [8–10]. In previous works [3–6], the good linearity of the impedance vs. RH curves is just appeared at the operating frequency of 100 Hz, while it of the KNN humidity sensor is appeared at the frequency range from 40 Hz to 1 kHz. Especially, the impedance changes of the KNN humidity sensor working at 60 Hz and 100 Hz are all about four orders of magnitude within the whole humidity range from 11% to 95% RH, which are larger than it working at 40 Hz and 1 kHz (the impedance only changes three orders of magnitude). The result indicates that the KNN humidity sensor is of lower operating frequency and wider working frequency range compared with previous work [4,5]. Therefore, the operating frequencies of 60 Hz and 100 Hz are applied in all investigations hereinafter.

Response and recovery behaviors are the significant characteristics for estimating the performance of humidity sensor. Fig. 5 shows the response and recovery properties of the KNN humidity sensor when the humidity changes from 11% to 95% RH and then returns to 11% RH. At the operating frequencies of 60 Hz and 100 Hz, the response times (as the humidity changes from 11% to 95% RH) are all approximately 8 s and the recovery times (as the humidity changes from 95% to 11% RH) are about 18 s, indicating that the KNN humidity sensor exhibits quick response–recovery properties to humidity from 11% RH to 95% RH. It should be noticed that the response time and recovery time of the KNN humidity sensor are almost the same when the operating frequencies are 60 Hz and 100 Hz, further indicating that the operating frequency of the

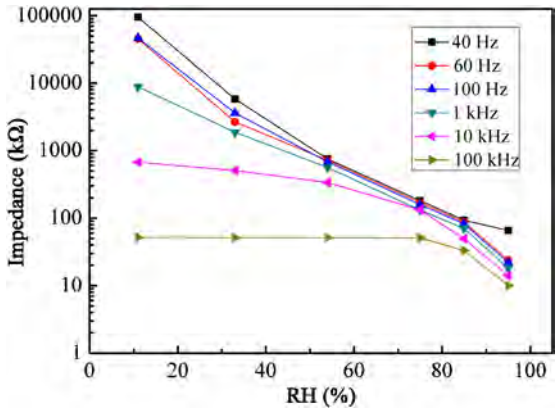

Fig. 4. Impedance vs. RH curves of the KNN humidity sensor at various frequencies.

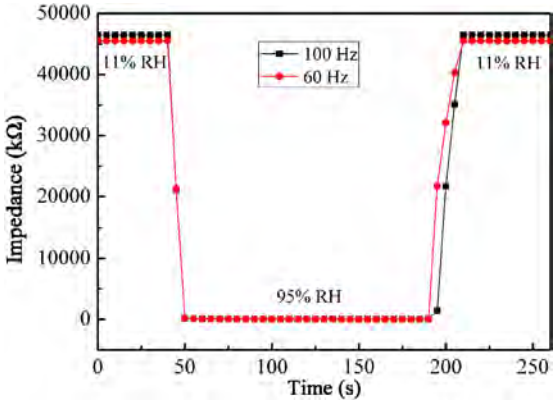

Fig. 5. Transient response characteristics of the KNN humidity sensor at 60 Hz and 100 Hz.

KNN humidity sensor is reduced and the working frequency range of it is broadened. Although the KNN humidity sensor is inevitably exposed to the laboratory atmosphere (about 25% RH) during the switching process, the switching time (about 1 s) is smaller than the response times (8 s) of the KNN humidity sensor. Therefore, the correctness of this experiment is acceptable, and it is consistent with the previous experiments [2,37,38].

Fig. 6 shows the humidity hysteresis properties of the KNN humidity sensor. The impedance of desorption process is slightly lower than that of adsorption process. Hence, the KNN humidity

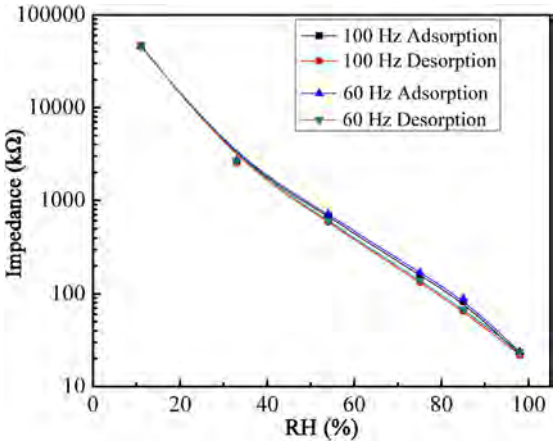

Fig. 6. Humidity hysteresis characteristic of the KNN humidity sensor measured at 60 Hz and 100 Hz.

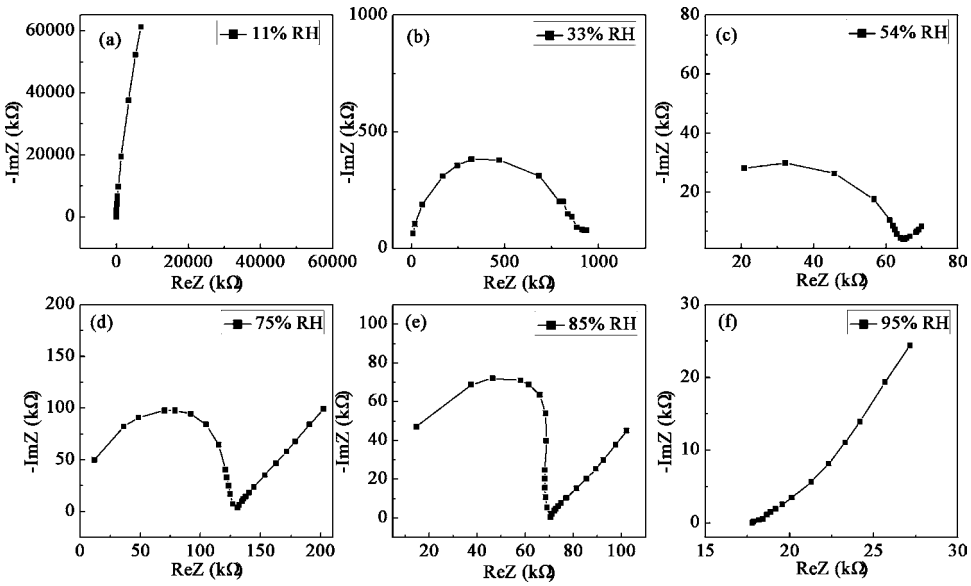

Fig. 7. The complex impedance plots of the KNN powder measured at (a) 11%, (b) 33%, (c) 54%, (d) 75%, (e) 85%, and (f) 95% RH in the frequency range from 40 Hz to 100 kHz.

sensor exhibits a narrow hysteresis loop during cyclic humidity operation. At 60 Hz and 100 Hz, the maximum humidity hystereses of the KNN humidity sensor are around 2% RH during the cyclic humidity operation, which illustrates that the KNN humidity sensor is of good reliability. The results indicate when the operating frequencies are 60 Hz and 100 Hz, the KNN humidity sensor has excellent properties such as good linearity, fast response speed and small humidity hysteresis. In summary, the KNN humidity sensor is of low operating frequency and wide working frequency range.

3.3. Discussion on the humidity sensing mechanism

To confirm the different adsorption mechanisms of humidity sensing materials at various RH values, complex impedance plots are adopted to interpret the conductivity and polarization processes that take place in a humidity sensor [39,40]. Complex impedance plots of the KNN humidity sensor at different RH values are measured over a frequency range of 40–100 kHz with a testing voltage of 1 V. Here, Re Z and Im Z are the real part and imaginary part of the complex impedance. The difference in the complex impedance plots implies different physical phenomena for the electrical conductivity and polarization that occur in the KNN humidity sensor. When the RH is low (11% RH), only an arc is observed, and the curvature radius is so large that it looks like a line as shown in Fig. 7(a). In Fig. 7(b)–(e), when the RH increases continually (33%, 54%, 75%, and 85% RH), the curvature radius of the arc reduces, and forms a depressed semicircle at high frequency which connects with a straight line at low frequency. The higher the RH is, the longer the line is. When the RH increases to 95% RH, the semicircle becomes invisible, only a straight line is left.

Based on the knowledge of dielectric physics theory [19], we know that the "resistor" represents the conduction process and the "capacitor" represents the polarization process in an equivalent circuit. At low RH levels (11% RH), the semicircle of the complex impedance plot represents a kind of humidity sensing mechanism, which can be modeled by an equivalent parallel circuit of a resistor and a capacitor [1,9]. According to the protons conductivity model of Anderson and Parks [41], when the RH is low, only a few water molecules are adsorbed and the surface is not completely covered. Therefore, the electrolytic conduction is difficult, only free protons can be formed and the conduction at room temperature is mainly due to the protons from site to site over energy barriers on the surface, resulting in high impedance of the KNN humidity sensor. When the RH increases continually (33%, 54%, 75%, 85% RH), one or several serial water layers are formed by physisorption. Since hydration of H_3O^+ is energetically favored in liquid water, we expect that H_3O^+ will be hydrated in the presence of sufficient adsorbed water [42]. According to the ion transfer mechanism of Grotthuss [43], $H_2O + H_3O^+ \rightarrow H_3O^+ + H_2O$, the initial and final states are the same, and the energy is also equivalent, so that the transfer of H_3O^+ is quite easy. On the other hand, according to the ion transport model of Casalbore-Miceli et al. [44], the KNN powder may dissolve in the adsorbed water, and the dissociated ions (Na^+ and K^+) can play the roles of conduction carriers. Hence the impedance of the KNN humidity sensor continuously decreases by about four orders of magnitude compared to the initial impedance with the increasing RH. Moreover, the semicircle connects with straight line, which means that the electrolytic conduction takes place in the adsorbed layers besides the protonic transport. When the RH increases to 95%, due to the active electrolytic conduction, the semicircle becomes ignorable [45], and the Warburg impedances caused by the diffusion of the electroactive species at the electrodes are represented as the lines in Fig. 7(f), which indicates that electrolytic conduction plays a predominant role.

Dielectric materials with high permittivity and low dielectric loss are widely required in different applications, such as humidity sensors, bypass capacitors in microelectronics and energy-storage devices [46–49]. Fig. 8 shows the dielectric dissipation factor (DF) vs. the frequency curves of the KNN humidity sensor at different RH. It can be seen that the DF of the KNN humidity sensor increases with the frequency increases, and the higher the RH is, the bigger the change of the DF is. When the frequency is high, the DF increases remarkably with the increase of the RH, while the DF is small and independent of the RH when the frequency is low. According to the theory of dielectrics physics, the DF represents the energy transformation resulting from the relaxation of the molecule polarization [50]. Dielectric polarization in a material is the sum total of the different polarization mechanisms, such as electronic, ionic (atom), dipolar and interfacial polarization [51,52].

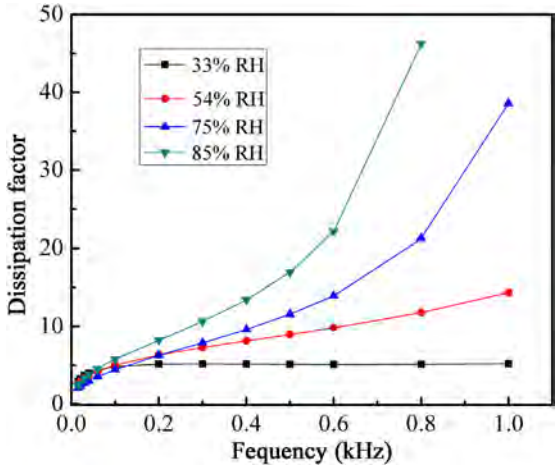

Fig. 8. The dielectric dissipation factor plots of the KNN humidity sensor.

According to capacitor equivalent circuit model, the magnitude of the DF can be represented by using the following expression [53]:

$$DF = DF_{if} + \left(\frac{2\pi f C R_{ESRhf}}{10000}\right) \quad (1)$$

where DF_{if} is represented with the percentage of the loss factor at low frequency, which is caused by power loss. The R_{ESRhf} is equivalent series resistance in the equivalent circuit, and f and C are the frequency and equivalent series capacitance, respectively. From the Eq. (1), the DF is linear to *f*, namely, the higher the *f* is, the larger the DF is. The leakage current is widely considered to be a major influential factor on the DF [54,55]. From Fig. 8, at the range of high working frequencies (100–800 Hz), the DF is high due to the large leakage current [55]. Especially, at the frequency of 800 Hz, the DF value is 46.23 at 85% RH, and the higher the frequency is, the larger the leakage current is [56,57]. At the frequency below 100 Hz, the value of the DF is low and independent of the RH, and the average DF values of the KNN humidity sensor are 4.61, 4.60, 4.00, 5.16 corresponding for 33%, 54%, 75%, 85% RH at the working frequency range of 60–100 Hz, respectively [55], indicating the KNN humidity sensor has good insulating properties at operating frequency [58]. Furthermore, as shown in Fig. 8, when the frequency is low, the DF is independent of the RH, namely, the deviation of humidity detection is small at the whole RH range, which indicates that the KNN humidity sensor is of good reliability.

4. Conclusion

In conclusion, the KNN powder is synthesized via MOD and its humidity sensing properties are investigated at different RH. At the frequencies of 60 Hz and 100 Hz, the KNN humidity sensor is of good linearity, and the variations of the KNN humidity sensor impedance are up to four orders of magnitude within the whole humidity range from 11% to 95% RH. The corresponding response time and recovery time are all about 8 s and 18 s, and their maximum hystereses are all around 2% RH at 60 Hz and 100 Hz. Furthermore, at low frequency conditions, the DF values of the KNN humidity sensor are small and independent of the RH, and the average DF values of the KNN humidity sensor are 4.61, 4.60, 4.00, 5.16 corresponding for 33%, 54%, 75%, 85% RH at the working frequency range of 60–100 Hz, respectively. The results suggest that the KNN powder has a potential application in fabricating high performance humidity sensors which are of low and wide working frequency range.

Acknowledgements

This work was supported by Scientific Research Fund of Hunan Provincial Education Department (14B168), PCSIRT (IRT1080), NNSF of China (51272158, 51402250) and Hunan Provincial Natural Science Foundation of China (2015JJ4046) .

References

[1] H.C. Bi, K.B. Yin, X. Xie, J. Ji, S. Wan, L.T. Sun, M. Terrones, M.S. Dresselhaus, Ultrahigh humidity sensitivity of graphene oxide, Sci. Rep. 3 (2013) 2714 (7 pp.).
[2] R. Wang, D. Wang, Y. Zhang, X.J. Zheng, Humidity sensing properties of $Bi_{0.5}(Na_{0.85}K_{0.15})_{0.5}Ti_{0.97}Zr_{0.03}O_3$ microspheres: effect of A and B sites co-substitution, Sens. Actuators B: Chem. 190 (2014) 305–310.
[3] L. Xu, R. Wang, Q. Xiao, D. Zhang, Y. Liu, Micro humidity sensor with high sensitivity and quick response/recovery based on ZnO/TiO_2 composite nanofibers, Chin. Phys. Lett. 28 (2011) 070702 (4 pp.).
[4] Y. Zhang, X.J. Zheng, T. Zhang, L.J. Gong, S.H. Dai, Y.Q. Chen, Humidity sensing properties of the sensor based on $Bi_{0.5}K_{0.5}TiO_3$ powder, Sens. Actuators B: Chem. 147 (2010) 180–184.
[5] Y. Zhang, X.J. Zheng, T. Zhang, Characterization and humidity sensing properties of $Bi_{0.5}Na_{0.5}TiO_3$-$Bi_{0.5}K_{0.5}TiO_3$ powder synthesized by metal-organic decomposition, Sens. Actuators B: Chem. 156 (2011) 887–892.
[6] J. Zhao, Y.P. Liu, X.W. Li, G.Y. Lu, L. You, X.S. Liang, F.M. Liu, T. Zhang, Y. Du, Highly sensitive humidity sensor based on high surface area mesoporous $LaFeO_3$ prepared by a nanocasting route, Sens. Actuators B 181 (2013) 802–809.
[7] Y. Zhang, X.J. Zheng, T. Zhang, J. Sun, Y. Bian, J. Song, Gas sensing properties of coral-like $Bi_{0.5}K_{0.5}TiO_3$ powders synthesized by metal-organic decomposition, Meas. Sci. Technol. 22 (2011) 115205 (6 pp.).
[8] Q. Qi, T. Zhang, X.J. Zheng, L.F. Wan, Preparation and humidity sensing properties of Fe-doped mesoporous silica SBA-15, Sens. Actuators B: Chem. 135 (2008) 255–261.
[9] J. Wang, B.K. Xu, S.P. Ruan, S.P. Wang, Preparation and electrical properties of humidity sensing films of $BaTiO_3$/polystrene sulfonic sodium, Mater. Chem. Phys. 78 (2003) 746–750.
[10] W.C. Geng, R. Wang, X.T. Li, Y.C. Zou, T. Zhang, J.C. Tu, Y. He, N. Li, Humidity sensitive property of Li-doped mesoporous silica SBA-15, Sens. Actuators B: Chem. 127 (2007) 323–329.
[11] H.B. Yang, Y. Lin, J.F. Zhu, F. Wang, An efficient approach for direct synthesis of $K_{0.5}Na_{0.5}NbO_3$ powders, Powder Technol. 196 (2009) 233–236.
[12] Y. Shiratori, A. Magrez, C. Pithan, Particle size effect on the crystal structure symmetry of $K_{0.5}Na_{0.5}NbO_3$, J. Eur. Ceram. Soc. 25 (2005) 2075–2079.
[13] T. Huang, D.Q. Xiao, C. Liu, F.X. Li, B. Wu, J.G. Wu, J.G. Zhu, Effect of $SrZrO_3$ on phase structure and electrical properties of 0.974 $(K_{0.5}Na_{0.5})NbO_3$–0.026 $Bi_{0.5}K_{0.5}TiO_3$ lead-free ceramics, Ceram. Int. 40 (2014) 2731–2735.
[14] L.Y. Wang, W. Ren, K. Yao, P. Shi, X.Q. Wua, X. Yao, Effects of thickness on structures and electrical properties of $K_{0.5}Na_{0.5}NbO_3$ thick films derived from polyvinylpyrrolidone-modified chemical solution, Ceram. Int. 38 (2012) 291–294.
[15] N. Li, W.L. Li, S.Q. Zhang, W.D. Fei, Effect of post-annealing treatment in oxygen on dielectric properties of $K_{0.5}Na_{0.5}NbO_3$ thin films prepared by chemical solution deposition, Thin Solid Films 519 (2011) 5070–5073.
[16] Y. Nakashima, W. Sakamoto, T. Yogo, Processing of highly oriented (K, Na)NbO_3 thin films using a tailored metal-alkoxide precursor solution, J. Eur. Ceram. Soc. 31 (2011) 2497–2503.
[17] B. Park, I. Hong, H. Jang, V. Tran, W. Tai, J. Lee, Highly enhanced mechanical quality factor in lead-free $(K_{0.5}Na_{0.5})NbO_3$ piezoelectric ceramics by co-doping with $K_{5.4}Cu_{1.3}Ta_{10}O_{29}$ and CuO, Mater. Lett. 64 (2010) 1577–1579.
[18] S.H. Qian, K.J. Zhun, X.M. Pang, J.S. Liu, J.H. Qiu, J.Z. Du, Phase transition, microstructure, and dielectric properties of Li/Ta/Sb co-doped (K, Na)NbO_3 lead-free ceramics, Ceram. Int. 40 (2014) 4389–4394.
[19] T. Zhang, R. Wang, W.C. Geng, X.T. Li, Q. Qi, Y. He, S.J. Wang, Study on humidity sensing properties based on composite materials of Li-doped mesoporous silica A-SBA-15, Sens. Actuators B: Chem. 128 (2008) 482–487.
[20] T. Fei, K. Jiang, S. Liu, T. Zhang, Humidity sensors based on Li-loaded nanoporous polymers, Sens. Actuators B: Chem. 190 (2014) 523–528.
[21] Y. Zhang, Y. Chen, Y.P. Zhang, X. Cheng, C.H. Feng, L.H. Chen, J.R. Zhou, S.P. Ruan, A novel humidity sensor based on $NaTaO_3$ nanocrystalline, Sens. Actuators B: Chem. 174 (2012) 485–489.
[22] Z.Y. Wang, C. Chen, T. Zhang, H.L. Guo, B. Zou, R. Wang, F.Q. Wu, Humidity sensitive properties of K^+-doped nanocrystalline $LaCo_{0.3}Fe_{0.7}O_3$, Sens. Actuators B: Chem. 126 (2007) 678–683.
[23] W.H. Hayt, Engineering Electromagnetics, seventh ed., McGraw Hill, New York, 2006.
[24] O. de la Barrière, C. Ragusa, C. Appino, F. Fiorillo, M. LoBue, F. Mazaleyrat, A computationally effective dynamic hysteresis model taking into account skin effect in magnetic laminations, Physica B 435 (2014) 80–83.
[25] T. Yu, K.W. Kwok, H.L.W. Chan, The synthesis of lead-free ferroelectric $Bi_{0.5}Na_{0.5}TiO_3$–$Bi_{0.5}K_{0.5}TiO_3$ thin films by sol–gel method, Mater. Lett. 61 (2007) 2117–2120.

[26] T. Yu, K.W. Kwok, H.L.W. Chan, Preparation and properties of sol–gel-derived $Bi_{0.5}Na_{0.5}TiO_3$ lead-free ferroelectric thin film, Thin Solid Films 515 (2007) 3563–3566.
[27] Q. Qi, T. Zhang, Y. Zeng, H.B. Yang, Humidity sensing properties of KCl-doped Cu—Zn/CuO—ZnO nanoparticles, Sens. Actuators B: Chem. 137 (2009) 21–26.
[28] L. Greenspan, Humidity fixed points of binary saturated aqueous solutions, J. Res. NBS 81A (1977) 89–96.
[29] S. Agarwal, G.L. Sharma, Humidity sensing properties of (Ba, Sr)TiO_3 thin films grown by hydrothermal–electrochemical method, Sens. Actuators B: Chem. 85 (2002) 205–211.
[30] J.H. Cho, J.B. Yu, J.S. Kim, S.O. Sohn, D.D. Lee, J.S. Huh, Sensing behaviors of polypyrrole sensor under humidity condition, Sens. Actuators B: Chem. 108 (2005) 389–392.
[31] X.J. Jiang, B.Y. Wang, L.H. Luo, W.P. Li, J. Zhou, H.B. Chen, Electrical properties of $(1-x)(Bi_{0.5}Na_{0.5})TiO_3$–$xKNbO_3$ lead-free ceramics, J. Solid State Chem. 213 (2014) 72–78.
[32] C.C. Chen, P. Liu, C.H. Lu, Synthesis and characterization of nano-sized ZnO powders by direct precipitation method, Chem. Eng. J. 144 (2008) 509–513.
[33] T. Rojac, M. Kosec, B. Malič, J. Holc, Mechanochemical synthesis of $NaNbO_3$, $KNbO_3$ and $K_{0.5}Na_{0.5}NbO_3$, Sci. Sinter. 37 (2005) 61–67.
[34] X.J. Zheng, S.H. Dai, X. Feng, T. Zhang, D.Z. Zhang, Y.Q. Gong, Y.Q. Chen, L. He, Structural and electrical properties of $(Na_{0.85}K_{0.15})_{0.5}Bi_{0.5}TiO_3$ thin films deposited on $LaNiO_3$ and Pt bottom electrodes, Appl. Surf. Sci. 256 (2010) 3316–3320.
[35] V. Bondarenka, S. Grebinskij, S. Mickevicius, V. Volkov, G. Zacharova, Thin films of poly-vanadium-molybdenum acid as starting materials for humidity sensors, Sens. Actuators B: Chem. 28 (1995) 227–231.
[36] P.M. Faia, C.S. Furtado, A.J. Ferreira, Humidity sensing properties of a thick-film titania prepared by a slow spinning process, Sens. Actuators B: Chem. 101 (2004) 183–190.
[37] Q. Qi, T. Zhang, Q.J. Yu, R. Wang, Y. Zeng, L. Liu, H.B. Yang, Properties of humidity sensing ZnO nanorods-base sensor fabricated by screen-printing, Sens. Actuators B: Chem. 133 (2008) 638–643.
[38] D. Bauskar, B.B. Kale, P. Patil, Synthesis and humidity sensing properties of $ZnSnO_3$ cubic crystallites, Sens. Actuators B: Chem. 161 (2012) 396–400.
[39] D.R. Saha, A. Datta, S. Mandal, M. Mukherjee, A.K. Nandi, D. Chakravorty, Nano-glass in lithia-silica system grown within pores of pellets comprising CuO nanoparticles, Solid State Ion. 186 (2011) 14–19.
[40] D.R. Saha, A.K. Nandi, D. Chakravorty, Enhancement of ionic conductivity in Li_2O—SiO_2 glass in nanodimensions grown within pellets of ZnO nanorods and magnetodielectric properties of these nanocomposites, J. Non-Cryst. Solids 376 (2013) 12–17.
[41] J.H. Anderson, G.A. Parks, The electrical conductivity of silica gel in the presence of adsorbed water, J. Phys. Chem. 72 (1968) 3662–3668.
[42] Q. Qi, Y.L. Feng, T. Zhang, X.J. Zheng, G.Y. Lu, Influence of crystallographic structure on the humidity sensing properties of KCl-doped TiO_2 nanofibers, Sens. Actuators B: Chem. 139 (2009) 611–617.
[43] F.M. Ernsberger, The nonconformist ion, J. Am. Ceram. Soc. 11 (1983) 747–750.
[44] G. Casalbore-Miceli, M.J. Yang, N. Camaioni, C.M. Mari, Y. Li, H. Sun, M. Ling, Investigations on the ion transport mechanism in conducting polymer films, Solid State Ion. 131 (2000) 311–321.
[45] B.M. Kulwicki, Humidity sensors, J. Am. Ceram. Soc. 74 (1991) 697–708.
[46] K. Yoo, M.J. Lee, K. Kwon, J. Jeong, N. Min, Dielectric properties of on-chip-cured polyimide films, Thin Solid Films 518 (2010) 5986–5991.
[47] Z.J. Wang, M.H. Cao, Z.H. Yao, Q. Zhang, Z. Song, W. Hu, Q. Xu, H. Hao, H.X. Liu, Z.Y. Yu, Giant permittivity and low dielectric loss of $SrTiO_3$ ceramics sintered in nitrogen atmosphere, J. Eur. Ceram. Soc. 34 (2014) 1755–1760.
[48] J. Oh, T. Moon, T.G. Kim, C. Kim, J.H. Lee, S.Y. Lee, B. Park, The dependence of dielectric properties on the thickness of (Ba, Sr)TiO_3 thin films, Curr. Appl. Phys. 7 (2007) 168–171.
[49] Y.Y. Li, P.F. Liang, X.L. Chao, Z.P. Yang, Preparation of $CaCu_3Ti_4O_{12}$ ceramics with low dielectric loss and giant dielectric constant by the sol–gel technique, Ceram. Int. 39 (2013) 7879–7889.
[50] J. Wang, X.H. Wang, X.D. Wang, Study on dielectric properties of humidity sensing nanometer materials, Sens. Actuators B: Chem. 108 (2005) 445–449.
[51] P. Palei, P. Kumar, D.K. Agrawal, Structural and electrical properties of microwave processed Ag modified KNN-LS ceramics, J. Microw. Power Electromagn. Energy 46 (2) (2012) 76–82.
[52] S. Swain, P. Kumar, D.K. Agrawal, Sonia, Dielectric and ferroelectric study of KNN modified NBT ceramics synthesized by microwave processing technique, Ceram. Int. 39 (2013) 3205–3210.
[53] Z.D. Zhao, High Voltage Engineering, China Electric Powder Press, Beijing, 1998.
[54] Y. Liu, G.S. Xu, J.F. Liu, D.F. Yang, X.X. Chen, Dielectric, piezoelectric properties of MnO_2-doped $(K_{0.5}Na_{0.5})NbO_3$–$0.05LiNbO_3$ crystal grown by flux-Bridgman method, J. Alloys Compd. 603 (2014) 95–99.
[55] J. Yuan, Z.L. Hou, H.J. Yang, Y. Li, Y.Q. Kang, W.L. Song, H.B. Jin, X.Y. Fang, M.S. Cao, High dielectric loss and microwave absorption behavior of multiferroic $BiFeO_3$ ceramic, Ceram. Int. 39 (2013) 7241–7246.
[56] P.T. Gautam, S.K. Singh, R.P. Tandon, Mechanism for leakage current conduction in manganese doped $Bi_{3.25}La_{0.75}Ti_3O_{12}$ (BLT) ferroelectric thin films, J. Alloys Compd. 606 (2014) 132–138.
[57] S. Karboyan, J.G. Tartarin, M. Rzin, L. Brunel, et al., Influence of gate leakage current on AlGaN/GaN HEMTs evidenced by low frequency noise and pulsed electrical measurements, Microelectron. Reliab. 53 (2013) 1491–1495.
[58] N. Kumar, A. Ghosh, R.N.P. Choudhary, Electrical behavior of $Pb(Zr_{0.52}Ti_{0.48})_{0.5}(Fe_{0.5}Nb_{0.5})_{0.5}O_3$ ceramics, Mater. Chem. Phys. 130 (2011) 381–386.

Biographies

Mengjiao Yuan entered the ME course in 2013, and majored in electronic science and technology, Xiangtan University, China.

Yong Zhang received his ME degree from the Faculty of Materials, Optoelectronics and Physics, Xiangtan University, China in 2007. He received his PhD in major of materials science and engineering in 2012 from Xiangtan University. Now, he is interested in the field of sensing functional materials, gas sensors and humidity sensors.

Xuejun Zheng received his MS degree in major of structure mechanics in 1989, and PhD degree in the field of fundamental mechanics in 2002 from Xiangtan University. He was appointed as a full professor in Faculty of Materials, Optoelectronics and Physics, Xiangtan University in 2003. Now, he is interested in the field of sensing functional materials, gas sensors and humidity sensors.

Bin Jiang entered the ME course in 2013, and majored in electronic science and technology, Xiangtan University, China.

Peiwen Li entered the ME course in 2013, and majored in electronic science and technology, Xiangtan University, China.

Shuifeng Deng received her bachelor's degree in major of semiconductor physics in 1978 from Wuhan University. Now she is appointed as a full professor in Faculty of Materials, Optoelectronics and Physics, Xiangtan University.